AIMS Mathematics, 10(5): 11732–11756.
DOI: 10.3934/math.2025531
Received: 20 March 2025
Revised: 03 May 2025
Accepted: 19 May 2025
Published: 21 May 2025

https://www.aimspress.com/journal/Math

Research article

Stability analysis of fractional two-dimensional reaction-diffusion model with applications in biological processes

Ishtiaq Ali[1,*] **and Saeed Islam**[2,*]

[1] Department of Mathematics and Statistics, College of Science, King Faisal University, P.O. Box 400, Al-Ahsa, 31982, Saudi Arabia

[2] Department of Mechanical Engineering, Prince Mohammad Bin Fahd University, P.O. Box 1664, Al Khobar 31952, Saudi Arabia

* **Correspondence:** Email: iamirzada@kfu.edu.sa (I. A.), sislam@pmu.edu.sa (S. I.).

Abstract: We study the stability of a two-dimensional fractional reaction-diffusion system under the Caputo differential operator in time. Our model is based on the Grey-Scott model, a well-known coupled reaction-diffusion system that describes the interaction between two chemical species. The diffusion term captures the species special spread, while the nonlinear term in the system describes the chemical reaction, resulting in a wide range of difficult, self-organizing patterns, including spots, stripes, or spirals, depending on the parameter values. We derive conditions for local stability of the homogeneous equilibrium by linearizing the system and analyzing the eigenvalues of the Jacobian. Furthermore, we construct appropriate Lyapunov functionals to establish global asymptotic stability of the discrete model under suitable conditions. This approach seeks to provide a robust framework for analyzing complex dynamical behaviors in systems governed by fractional-order in-time reaction-diffusion systems. The numerical simulations employ the Chebyshev spectral method for spatial discretization and the $L1$ scheme for fractional time derivatives. These simulations validate the theoretical findings, demonstrating the model's ability to replicate intricate patterns often observed in reaction-diffusion systems. The results suggest that the fractional-order framework enhances the understanding of pattern formation in such systems, making this model a valuable tool for studying anomalous diffusion and non-local dynamics in biological and chemical processes.

Keywords: fraction reaction-diffusion system in 2D; biological processes; local and global stability; spectral method; Lyapunov method; numerical simulations
Mathematics Subject Classification: 35K57, 35R11, 35B35, 37M05

1. Introduction

Reaction-diffusion systems (RDS) are essential for understanding various natural processes, particularly in biology, chemistry, and physics. These systems are described by partial differential equations (PDEs) that combine two primary components: A reaction term and a diffusion term. The reaction term governs the local dynamics, such as chemical reactions or biological interactions, while the diffusion term represents the spatial movement of substances like chemicals or species. In biology, RDS models are used to describe pattern formation, tissue growth, and other biological processes where spatial and temporal changes occur due to reactions and diffusion [1, 2]. The significance of reaction-diffusion equations is particularly notable in their ability to capture the emergence of complex patterns, such as stripes, spots, and spirals, seen in biological and chemical systems. For instance, in the pioneering work of Turing, the role of RDS in explaining morphogenesis, the process by which organisms develop their shape, was established. This theory has since been applied to a wide range of scientific disciplines, including ecology, where these equations model population dispersal, and chemistry, where they help explain autocatalytic reactions [3, 4].

In his classical 1952 paper, Turing proposed a potential link between the patterns observed in biological systems and those that could spontaneously emerge in chemical reaction-diffusion systems. His work spurred extensive theoretical research into mathematical models of pattern formation. However, Turing-type patterns were not observed in controlled laboratory settings until the early 1990s. Since then, there has been renewed interest in chemical pattern formation and its connection to the strikingly similar patterns seen across various physical and biological systems. Recent numerical simulations of a simple chemical model have revealed spot patterns that continuously undergo 'birth' through replication and 'death' due to overcrowding. Here, we present laboratory experiments on the ferrocyanide-iodate-sulphite reaction, demonstrating similar behavior. The repeated growth and replication of these spots can be observed under a wide range of conditions and replicated by a simple two-species model, indicating that such replicating patterns may be a common feature in many reaction-diffusion systems [5–8].

RDS systems are highly nonlinear, making analytical solutions challenging to obtain. As a result, numerical methods have become crucial in solving these models, particularly in cases where complex spatio-temporal behaviors arise. The patterns generated by these equations often exhibit features such as Turing instability, where small perturbations lead to the formation of distinct spatial structures, further highlighting the broad application of RDS in understanding natural phenomena [9, 10]. Various computational techniques have been proposed in the literature to solve non-linear reaction-diffusion models associated with pattern formation. For instance, Ersoy developed an algorithm using exponential cubic B-splines to study these equations [11]. Onarcan et al. introduced a method based on trigonometric cubic B-splines for solving these models [12]. Additionally, finite difference methods and the finite element method have been employed to address these models in [13–15]. Mittal and his co-author used a modified cubic B-spline approach combined with differential quadrature to solve RDS [16].

The Gray-Scott model is a modified version of the autocatalytic model that was initially introduced as a refinement of the autocatalytic Selkov model proposed by Selkov. This model is based on autocatalytic reactions, where one of the reactants facilitates its own production, leading to rich and complex behaviors. Specifically, the Gray-Scott model captures the dynamics of two chemical species,

typically denoted as $\mathcal{U}$ (the reactant) and $\mathcal{V}$ (the autocatalyst), which participate in autocatalytic reactions [17–20]. The governing chemical reactions are as follows:

$$\mathcal{U} + 2\mathcal{V} \to 3\mathcal{V},$$

$$\mathcal{V} \to \mathcal{P},$$

which occurs in an open flow reactor where the reactant $\mathcal{U}$ is continuously supplied and the product $\mathcal{P}$ is removed. The first reaction depicts an autocatalytic process where two molecules of species $\mathcal{V}$ interact with one molecule of species $\mathcal{U}$ to produce three molecules of $\mathcal{V}$. The second reaction represents the decay of $\mathcal{V}$ into the product $\mathcal{P}$.

In a closed system, these two irreversible processes would eventually convert all the reactants into the product. However, by maintaining a continuous feed of species $\mathcal{U}$ while removing the product and excess reactants, far-from-equilibrium conditions can be sustained. This setup enables the emergence of various instabilities and complex nonlinear dynamics.

These systems can be collected into a general form:

$$\begin{aligned} u_t &= \nu_1 \Delta u + \mathcal{A}_1 u + \mathcal{B}_1 v - \mathcal{F}(u,v) + \mathcal{G}_1(x,y,u,v), \\ v_t &= \nu_2 \Delta v + \mathcal{A}_2 u + \mathcal{B}_2 v + \mathcal{F}(u,v) + \mathcal{G}_2(x,y,u,v), \quad (x,y) \in \Omega. \end{aligned} \tag{1.1}$$

In the reaction-diffusion system given by Eq (2.2), the variables $u(x,y,t)$ and $v(x,y,t)$ represent the spatiotemporal concentrations (or densities) of two interacting species over time t. The coefficients ν_1 and ν_2 are the positive diffusion coefficients associated with species u and v, respectively, and Δ denotes the Laplacian operator, modeling the spatial diffusion process in the domain. The terms $\mathcal{A}_1 u$ and $\mathcal{B}_1 v$ represent linear reaction kinetics for the evolution of u, while $\mathcal{A}_2 u$ and $\mathcal{B}_2 v$ serve similar roles for the dynamics of v. The nonlinear term $\mathcal{F}(u,v)$ models the coupled nonlinear interaction between the species, such as production, inhibition, or consumption processes. The functions $\mathcal{G}_1(x,y,u,v)$ and $\mathcal{G}_2(x,y,u,v)$ account for external forcing, spatial heterogeneities, or inhomogeneous source effects, which may arise from continuous feeding of reactants or removal of products to maintain the system far from equilibrium.

The most common reaction-diffusion models based on the parameter values in the model equation (2.2) are

- **Gray–Scott**: $\mathcal{A}_1 = -P < 0, \quad \mathcal{B}_1 = 0, \quad \mathcal{A}_2 = 0, \quad \mathcal{B}_2 = (-P + \delta) < 0, \quad \mathcal{F} = uv^2, \quad \mathcal{G}_1 = P, \quad \mathcal{G}_2 = 0.$
- **Brusselator**: $\mathcal{A}_1 = 0, \quad \mathcal{B}_1 = \mathcal{B}, \quad \mathcal{A}_2 = 0, \quad \mathcal{B}_2 = -(\mathcal{B} + 1) < 0, \quad \mathcal{F} = uv^2, \quad \mathcal{G}_1 = 0, \quad \mathcal{G}_2 = \mathcal{A}.$
- **Glycolysis**: $\mathcal{A}_1 = -\delta < 0, \quad \mathcal{B}_1 = 0, \quad \mathcal{A}_2 = \delta, \quad \mathcal{B}_2 = -1, \quad \mathcal{F} = uv^2, \quad \mathcal{G}_1 = \xi, \quad \mathcal{G}_2 = 0.$

We are more interested in the dynamics of the Grey-Scott model. After appropriate rescaling and the inclusion of diffusion and using the above parameter values, the governing equations in two dimensions with a fractional in-time version of the reaction equation (2.2) can be expressed as

$$\begin{aligned} {}_{C_0}\mathcal{D}_t^{\alpha} u(x,y,t) &= \nu_1 \left(\frac{\partial^2 u}{\partial x^2} + \frac{\partial^2 u}{\partial y^2} \right) - uv^2 + P(1-u), \\ {}_{C_0}\mathcal{D}_t^{\alpha} v(x,y,t) &= \nu_2 \left(\frac{\partial^2 v}{\partial x^2} + \frac{\partial^2 v}{\partial y^2} \right) + uv^2 - (P+\delta)v, \quad (x,y) \in \Omega, \quad t > 0, \end{aligned} \tag{1.2}$$

subject to zero flux boundary conditions of the form:

$$\frac{\partial u}{\partial n} = \frac{\partial v}{\partial n} = 0 \quad \text{on} \quad \partial\Omega$$

where $\frac{\partial}{\partial n}$ represents the derivative in the direction normal to the boundary $\partial\Omega$. The initial conditions for the system are defined as:

$$u(x, y, 0) = \phi_1(x, y), \quad v(x, y, 0) = \phi_2(x, y),$$

where $\phi_1(x, y)$ and $\phi_2(x, y)$ are the initial profiles for u and v.

In model equation (1.2), ${}_{C_0}\mathcal{D}_t^{\alpha}$ denotes the Caputo fractional derivative, $u(x, y, t)$ and $v(x, y, t)$ are the concentrations of species $\mathcal{U}$ and $\mathcal{V}$, respectively, ν_1 and ν_2 are the diffusion coefficients of u and v, P is the feed rate of the reactant $\mathcal{U}$, δ is the decay rate of $\mathcal{V}$, uv^2 represents the autocatalytic reaction where $\mathcal{U}$ catalyzes the production of more v, and $P(1 - u)$ is the replenishment term for u, which ensures that the reactant is fed into the system.

The Gray-Scott model has gained prominence due to its ability to produce a variety of intricate spatio-temporal patterns, such as stripes, spots, and wavefronts. These patterns are sensitive to the choice of system parameters, leading to phenomena such as Turing patterns and chaos. As a result, the model has become a key tool for studying pattern formation in chemical reactions and has applications in understanding processes such as morphogenesis, where biological structures arise from seemingly homogeneous environments. In addition to its classical integer-order form, the Gray-Scott model has been extended to incorporate fractional derivatives, allowing for the exploration of anomalous diffusion and other non-classical transport phenomena. This extension further enriches the study of pattern formation, as it introduces new dynamical behaviors that are not present in the integer-order version of the model [21, 22].

The Gray-Scott model with fractional derivatives in time offers a significant advancement over the classical model by incorporating fractional-order time derivatives, which better capture the memory effects and non-local temporal dynamics present in many real-world systems. In traditional reaction-diffusion models, the time evolution of concentrations is governed by integer-order derivatives, which assume that the system's future state depends only on its current state. However, many processes, particularly in biology, chemistry, and materials science, exhibit long-term memory, where the system's history influences its current and future behavior [23, 24].

By introducing fractional time derivatives (often in the Caputo or Riemann-Liouville sense), the Gray-Scott model becomes more flexible in modeling complex temporal behaviors, allowing the reaction rates and diffusion to depend on past states over a continuum of time. This makes it especially useful for modeling processes such as chemical autocatalysis or biological pattern formation, where the speed of reactions or diffusion is influenced by events in the system's history. The inclusion of fractional time derivatives also enables the model to describe anomalous temporal dynamics, such as sub-diffusion (slower than normal diffusion) or super-diffusion (faster than normal diffusion), which are observed in processes like molecular diffusion in cells or reactive transport in porous media. The ability to fine-tune the order of the time derivative allows researchers to capture a wide range of temporal behaviors that would be impossible to model accurately with integer-order derivatives alone.

A lot of work has been done to study the pattern formation of systems governed by fractional dynamics. For example, Owolabi et al. proposed a Fourier spectral method to investigate complex

Turing patterns emerging from autocatalytic reactions, utilizing the Caputo fractional derivative [25]. Alqhtani et al. explored spatiotemporal and chaotic patterns in fractional-order prey-predator models, while further work by Alqhtani and collaborators examined the formation of spatiotemporal patterns in predator-prey models through local and global stability analysis using Caputo fractional derivatives [26, 27]. Other authors presented various pattern formation scenarios in super-diffusive systems involving the Caputo operator [28]. Additionally, Owolabi et al. developed a mathematical model incorporating fractional-order super-diffusive processes to study emergent pattern formation in predator-prey systems [29]. Owolabi and Baleanu described the emergence of several patterns in diffusive Turing-like models with a fractional operator [30]. In another study, the spatial patterns of modified prey-predator systems were analyzed through diffusion-driven instability and associated chaotic behaviors [31]. Owolabi and Patidar also discussed high-order solution strategies for stiff time-dependent partial differential equations and their spatiotemporal dynamics in reaction-diffusion systems [32]. Owolabi explored the pattern formation in various fractional reaction-diffusion systems, while Pindza and Owolabi implemented a numerical scheme combining Fourier spectral methods for space and an exponential integrator for time to solve space-fractional reaction-diffusion equations [33, 34].

Recent studies have shown that the Gray-Scott model exhibits self-reproducing spots in two dimensions [35, 36]. A region (or interval) is roughly characterized as a two-dimensional point (or a one-dimensional pulse) where the concentrations largely resemble the globally stable homogeneous steady state outside of that region (or interval). Extensive research has been conducted on the fractional Gray-Scott reaction-diffusion model. For instance, because the exact solutions to the fractional Gray-Scott system are not known, second-order numerical methods have been explored to solve the equations. The conventional approach for solving fractional diffusion equations involves discretizing the fractional derivatives using finite difference or finite element methods, followed by applying the Euler scheme for time integration [37–41]. The global dynamics of nonlinear viscoelastic systems and the asymptotic behavior of damped generalized Ostrovsky equations have been rigorously analyzed, highlighting conditions for global existence, blow-up, and long-time decay of solutions below the energy space. The analysis is further supported by the construction of appropriate Lyapunov functions, which play a crucial role in establishing stability, decay estimates, and long-time behavior of solutions in both viscoelastic and damped wave models [42, 43]. The stability analysis of nonlinear fractional differential systems with delay has been advanced using Lyapunov-based methods, where sufficient conditions for asymptotic and exponential stability are derived through both Lyapunov functionals and Razumikhin-type approaches. Additionally, the generalized Mittag-Leffler stability framework has been introduced to extend the classical Lyapunov direct method for fractional-order nonlinear dynamic systems, offering broader criteria for stability verification. Furthermore, sufficient conditions for both local and global Lyapunov stability of nonlinear fractional-order systems have been established using Caputo derivatives, contributing to the theoretical understanding and practical analysis of fractional dynamic models [44–46].

The primary aim of this study is to introduce the fractional Gray-Scott reaction-diffusion model and conduct a comprehensive investigation into its dynamics, including the local asymptotic stability and global stability of constant positive equilibria using the discrete version of the proposed model. We further explore how discretization and non-integer orders influence the model. For numerical simulation to further validate our theoretical results, we use a Chebyshev spectral method in space,

while $L1$ is used for fractional-in-time derivatives. For more details about spectral methods, we refer the reader to [47–54]. The choice of the Chebyshev spectral method and the $L1$ scheme is motivated by the nature of the problem under investigation. The Grey-Scott model with fractional time derivatives involved nonlocal memory effects, sharp spatial gradients, and complex pattern formation, which demand high spatial resolution and numerical accuracy. The Chebyshev spectral method is well-suited for such problems due to its spectral convergence when the solution is sufficiently smooth, offering superior accuracy compared to low-order methods, especially on bounded domains with homogeneous Neumann (zero-flux) boundary conditions. Furthermore, the $L1$ scheme is a widely accepted method for discretizing Caputo fractional derivatives; it is simple to implement, stable, and accurate.

The rest of this paper is organized as follows: In Section 2, we analyze the local stability, while the global stability of the proposed fractional discrete Gray-Scott model is presented in Section 3. The detailed method description for numerical simulations is presented in Section 4, followed by a results and discussion in Section 5 to confirm the theoretical justifications.

2. Local stability

To perform the stability analysis of the model equation (1.2), we consider its discrete counterpart, since in biological processes the data are often discrete and more practical than the continuous form. Let the time grid be $t_n = nh,\ n \in \mathbb{N}$, where $h > 0$ is the time step size and $t \in (h\mathbb{N})_{t_0}$. The second-order spatial derivatives are approximated using central differences. Then, the discrete form of the fractional-in-time reaction-diffusion system becomes:

$$\begin{aligned} C_h\nabla^{\alpha}_{t_0}u_{i,j}(t) &= \nu_1\left(\frac{1}{h_x^2}\Delta_x^2 u_{i,j}(t+\alpha h) + \frac{1}{h_y^2}\Delta_y^2 u_{i,j}(t+\alpha h)\right) \\ &\quad - u_{i,j}(t)\, v_{i,j}^2(t+\alpha h) + P\left(1 - u_{i,j}(t+\alpha h)\right), \\ C_h\nabla^{\alpha}_{t_0}v_{i,j}(t) &= \nu_2\left(\frac{1}{h_x^2}\Delta_x^2 v_{i,j}(t+\alpha h) + \frac{1}{h_y^2}\Delta_y^2 v_{i,j}(t+\alpha h)\right) \\ &\quad + u_{i,j}(t+\alpha h)\, v_{i,j}^2(t+\alpha h) - (P+\delta)\, v_{i,j}(t+\alpha h), \end{aligned} \tag{2.1}$$

subject to appropriate initial and boundary conditions.

2.1. Local stability without diffusion

In this section, we analyze the local stability of the discrete version of the fractional reaction-diffusion model given in Eq (2.1) without the spatial diffusion terms. This means we focus only on the reaction dynamics. The discrete form of the system without diffusion becomes:

$$\begin{aligned} C_h\nabla^{\alpha}_{t_0}u(t) &= -u(t)\, v^2(t+\alpha h) + P\left(1 - u(t+\alpha h)\right), \\ C_h\nabla^{\alpha}_{t_0}v(t) &= u(t+\alpha h)\, v^2(t+\alpha h) - (P+\delta)\, v(t+\alpha h). \end{aligned} \tag{2.2}$$

To analyze the stability, we first determine the equilibrium points (u^*, v^*) by solving the system at steady state:

$$\begin{aligned} -u^* v^{*2} + P(1-u^*) &= 0, \\ u^* v^{*2} - (P+\delta)v^* &= 0. \end{aligned} \tag{2.3}$$

Solving this system, if $(P+\delta)^2 < P$, then there exist three equilibrium points:

$$\begin{aligned}(u_0^*, v_0^*) &= (1, 0),\\ (u_1^*, v_1^*) &= \left(\frac{2\eta}{P+\sigma}, \frac{P+\sigma}{2\eta}\right),\\ (u_2^*, v_2^*) &= \left(\frac{2\eta}{P-\sigma}, \frac{P-\sigma}{2\eta}\right),\end{aligned} \tag{2.4}$$

where $\sigma = \sqrt{P^2 - 4P\eta^2}$ and $\eta = P + \delta$.

Next, we define the reaction functions:

$$\begin{aligned}\varphi(u, v) &= -uv^2 + P(1-u),\\ \psi(u, v) &= uv^2 - (P+\delta)\, v.\end{aligned} \tag{2.5}$$

The Jacobian matrix of the system evaluated at an equilibrium point is:

$$\mathcal{J}(u, v) = \begin{pmatrix} \frac{\partial\varphi}{\partial u} & \frac{\partial\varphi}{\partial v} \\ \frac{\partial\psi}{\partial u} & \frac{\partial\psi}{\partial v} \end{pmatrix}. \tag{2.6}$$

The partial derivatives are:

$$\begin{aligned}\frac{\partial\varphi}{\partial u} &= -v^2 - P, \quad \frac{\partial\varphi}{\partial v} = -2uv,\\ \frac{\partial\psi}{\partial u} &= v^2, \quad \frac{\partial\psi}{\partial v} = 2uv - \eta.\end{aligned}$$

Thus, the Jacobian matrix at the equilibrium point (u^*, v^*) is:

$$\mathcal{J}(u^*, v^*) = \begin{pmatrix} -v^{*2} - P & -2u^*v^* \\ v^{*2} & 2u^*v^* - (P+\delta) \end{pmatrix}. \tag{2.7}$$

Theorem 1. The conditions for local stability at the equilibrium points (u^*, v^*) of the system given by (2.2) are:

- For the equilibrium point $(u_0^*, v_0^*) = (1, 0)$, if $P > 0$ and $\eta > 0$, then it is locally asymptotically stable.
- For the equilibrium point (u_1^*, v_1^*), it is locally asymptotically stable if either of the following conditions holds:

  (1) If
  $$\frac{(P^2+P\eta)(P^2+P\eta+4\eta^2(\eta-2)-2\eta^3)+4\eta^4((\eta-2)^2+8P)}{4\eta^4} > 0,$$
  $$\frac{P^2+P\eta}{2\eta^2}\cdot\eta > 2P, \quad \text{and} \quad \frac{-P^2+P\eta}{2\eta^2} - \eta + 2 < 0.$$

  (2) Or if
  $$\frac{(P^2+P\eta)(P^2+P\eta+4\eta^2(\eta-2)-2\eta^3)+4\eta^4((\eta-2)^2+8P)}{4\eta^4} \le 0,$$
  $$\frac{P^2+P\eta}{2\eta^2}\cdot\eta < 2P, \quad \text{and} \quad \frac{-P^2+P\eta}{2\eta^2} - \eta + 2 \le 0.$$

- The system is locally asymptotically stable at the equilibrium point (u_2^*, v_2^*) if one of the following holds:

  (1) If
  $$\frac{(P^2 - P\eta)(P^2 - P\eta + 4\eta^2(\eta - 2) - 8\eta^3) + 4\eta^4(\eta(\eta - 2)^2 + 8P)}{4\eta^4} > 0,$$
  $$\frac{P^2 - P\eta}{2\eta^2} \cdot \eta > 2P, \quad \text{and} \quad \frac{-P^2 - P\eta}{2\eta^2} - \eta + 2 < 0.$$

  (2) Or if
  $$\frac{(P^2 - P\eta)(P^2 - P\eta + 4\eta^2(\eta - 2) - 8\eta^3) + 4\eta^4(\eta(\eta - 2)^2 + 8P)}{4\eta^4} \leq 0,$$
  $$\frac{P^2 - P\eta}{2\eta^2} \cdot \eta > 2P, \quad \text{and} \quad \frac{-P^2 - P\eta}{2\eta^2} - \eta + 2 \leq 0.$$

Proof. We analyze the local stability at each equilibrium point using the Jacobian matrix.

- For $(u_0^*, v_0^*) = (1, 0)$, the Jacobian matrix is
  $$\mathcal{J}(u_0^*, v_0^*) = \begin{pmatrix} -P & 0 \\ 0 & -\eta \end{pmatrix}.$$
  The characteristic equation is
  $$(\lambda + P)(\lambda + \eta) = 0,$$
  with eigenvalues
  $$\lambda_1 = -P, \quad \lambda_2 = -\eta.$$
  Since both are negative when $P, \eta > 0$, the equilibrium point is locally asymptotically stable.
- For (u_1^*, v_1^*), the Jacobian matrix is
  $$\mathcal{J}(u_1^*, v_1^*) = \begin{pmatrix} \dfrac{-P^2 + P\eta}{2\eta^2} & -2 \\ \dfrac{P^2 + P\eta}{2\eta^2} & -P^2 - \eta \end{pmatrix}.$$
  The trace and determinant are
  $$\text{tr} = \frac{-P^2 + P\eta}{2\eta^2} - \eta + 2, \quad \det = \frac{P^2 + P\eta}{2\eta^2} \cdot \eta - 2P.$$
  The discriminant of the characteristic polynomial is:
  $$\Delta_1 = (\text{tr})^2 - 4 \cdot \det = \frac{(P^2 + P\eta)(P^2 + P\eta + 4\eta^2(\eta - 2) - 2\eta^3) + 4\eta^4((\eta - 2)^2 + 8P)}{4\eta^4}.$$
  The system is locally asymptotically stable if either:
  - $\Delta_1 > 0$, $\det > 0$, and $\text{tr} < 0$, or
  - $\Delta_1 < 0$ with eigenvalues having negative real parts.

- For (u_2^*, v_2^*), the Jacobian matrix is

$$\mathcal{J}(u_2^*, v_2^*) = \begin{pmatrix} \dfrac{-P^2 + P\eta}{2\eta^2} & -2 \\ \dfrac{P^2 - P\eta}{2\eta^2} & -P^2 - \eta \end{pmatrix}.$$

Its trace and determinant are:

$$\text{tr} = \frac{-P^2 + P\eta}{2\eta^2} - \eta + 2, \quad \det = \frac{P^2 - P\eta}{2\eta^2} \cdot \eta - 2P,$$

and the discriminant is:

$$\Delta_2 = \frac{(P^2 - P\eta)(P^2 - P\eta + 4\eta^2(\eta - 2) - 8\eta^3) + 4\eta^4(\eta(\eta - 2)^2 + 8P)}{4\eta^4}.$$

As before, the system is locally asymptotically stable if: $\Delta_2 > 0$, det > 0, and tr < 0, or $\Delta_2 < 0$, and eigenvalues have negative real parts.

2.2. *Stability analysis with diffusion*

To analyze the linear stability of system (2.1) with diffusion, we consider small perturbations around the steady state of the form:

$$u_{i,j}(t) = u^* + \epsilon\tilde{u}_{i,j}(t), \quad v_{i,j}(t) = v^* + \epsilon\tilde{v}_{i,j}(t), \quad 0 < \epsilon \ll 1,$$

and linearize the system by retaining only the first-order terms in ϵ. The discrete Laplacians satisfy the eigenvalue problem:

$$\left(\frac{1}{h_x^2}\Delta_x^2 + \frac{1}{h_y^2}\Delta_y^2\right)\phi_{i,j} = -\theta_{i,j}\phi_{i,j},$$

where $\theta_{i,j}$ are eigenvalues associated with spatial modes $\phi_{i,j}$. Substituting the perturbations into (2.1), the linearized system becomes:

$$\begin{aligned} C_h\nabla_{t_0}^{\alpha}\tilde{u}_{i,j}(t) &= -\nu_1\theta_{i,j}\tilde{u}_{i,j}(t + \alpha h) - v^{*2}\tilde{u}_{i,j}(t + \alpha h) - 2u^*v^*\tilde{v}_{i,j}(t + \alpha h) - P\tilde{u}_{i,j}(t + \alpha h), \\ C_h\nabla_{t_0}^{\alpha}\tilde{v}_{i,j}(t) &= -\nu_2\theta_{i,j}\tilde{v}_{i,j}(t + \alpha h) + v^{*2}\tilde{u}_{i,j}(t + \alpha h) + 2u^*v^*\tilde{v}_{i,j}(t + \alpha h) - (P + \delta)\tilde{v}_{i,j}(t + \alpha h). \end{aligned} \tag{2.8}$$

This system can be written in compact matrix form as:

$$C_h\nabla_{t_0}^{\alpha}\mathbf{W}_{i,j}(t) = \mathbf{J}_{\theta_{i,j}}(u^*, v^*)\,\mathbf{W}_{i,j}(t + \alpha h), \tag{2.9}$$

where the perturbation vector is:

$$\mathbf{W}_{i,j}(t) = \begin{pmatrix} \tilde{u}_{i,j}(t) \\ \tilde{v}_{i,j}(t) \end{pmatrix},$$

and the Jacobian matrix evaluated at equilibrium (u^*, v^*) is:

$$\mathbf{J}_{\theta_{i,j}}(u^*, v^*) = \begin{pmatrix} -\nu_1\theta_{i,j} - v^{*2} - P & -2u^*v^* \\ v^{*2} & -\nu_2\theta_{i,j} + 2u^*v^* - (P + \delta) \end{pmatrix}.$$

Theorem 2. The diffusion-included system is asymptotically stable at the equilibrium point (u^*, v^*) if the following conditions hold:

- The point $(u_0^*, v_0^*) = (1, 0)$ is asymptotically stable if:

$$\frac{\nu_1}{\delta^2}\theta_i - P < 0, \quad \text{and} \quad \frac{\nu_2}{\delta^2}\theta_i - (P + \delta) < 0.$$

- The point (u_1^*, v_1^*) is asymptotically stable if the following conditions hold:

(1) If

$$-\frac{2\nu_1\nu_2}{\delta^4} \cdot \frac{P^2 + P\sigma}{2\eta^2}(-\eta + 2) > \left(\frac{\nu_1 - \nu_2}{\delta^2}\right)^2 \Delta, \quad \text{and} \quad \frac{\nu_1}{\delta^2}\theta_i - \frac{P^2 + P\sigma}{2\eta^2} \geq 0,$$

then the eigenvalues

$$\lambda_j(\theta_i) = \frac{\mathrm{tr}(J_i^*) \pm \sqrt{\mathrm{tr}(J_i^*)^2 - 4\det(J_i^*)}}{2}, \quad j = 1, 2,$$

satisfy $\mathrm{Arg}(\lambda_j(\theta_i)) > \frac{\xi\pi}{2}$.

(2) If

$$-\frac{2\nu_1\nu_2}{\delta^4} \cdot \frac{P^2 + P\sigma}{2\eta^2}(-\eta + 2) < \left(\frac{\nu_1 - \nu_2}{\delta^2}\right)^2 \Delta,$$

then the eigenvalues are complex:

$$\lambda_j(\theta_i) = \frac{\mathrm{tr}(J_i^*)}{2} \pm i\frac{\sqrt{-\Delta}}{2}, \quad j = 1, 2,$$

and must satisfy $\mathrm{Arg}(\lambda_j(\theta_i)) > \frac{\xi\pi}{2}$.

- The point (u_2^*, v_2^*) is asymptotically stable if the following conditions hold:

(1) If

$$-\frac{2\nu_1\nu_2}{\delta^4} \cdot \frac{P^2 - P\sigma}{2\eta^2}(-\eta + 2) > \left(\frac{\nu_1 - \nu_2}{\delta^2}\right)^2 \Delta^*, \quad \text{and} \quad \frac{\nu_1}{\delta^2}\theta_i - \frac{P^2 - P\sigma}{2\eta^2} \geq 0,$$

then the eigenvalues

$$\lambda_j(\theta_i) = \frac{\mathrm{tr}(J_i^*) \pm \sqrt{\mathrm{tr}(J_i^*)^2 - 4\det(J_i^*)}}{2}, \quad j = 1, 2,$$

satisfy $\mathrm{Arg}(\lambda_j(\theta_i)) > \frac{\xi\pi}{2}$.

(2) If

$$-\frac{2\nu_1\nu_2}{\delta^4} \cdot \frac{P^2 - P\sigma}{2\eta^2}(-\eta + 2) < \left(\frac{\nu_1 - \nu_2}{\delta^2}\right)^2 \Delta^*,$$

then the eigenvalues are complex:

$$\lambda_j(\theta_i) = \frac{\mathrm{tr}(J_i^*)}{2} \pm i\frac{\sqrt{-\Delta^*}}{2}, \quad j = 1, 2,$$

and must satisfy $\mathrm{Arg}(\lambda_j(\theta_i)) > \frac{\xi\pi}{2}$.

Proof. We analyze the linear stability of the system (2.1) by studying the behavior of small perturbations around each equilibrium point. The linearized system can be written as:

$$C_h \nabla_{t_0}^{\alpha} \mathbf{W}_{i,j}(t) = \mathbf{J}_{\theta_{i,j}}(u^*, v^*)\, \mathbf{W}_{i,j}(t + \alpha h),$$

where $\mathbf{W}_{i,j}(t) = \begin{pmatrix} \tilde{u}_{i,j}(t) \\ \tilde{v}_{i,j}(t) \end{pmatrix}$ and $\mathbf{J}_{\theta_{i,j}}(u^*, v^*)$ is the Jacobian matrix evaluated at the steady state (u^*, v^*), incorporating diffusion via the eigenvalue $\theta_{i,j}$.

We now analyze the stability at each equilibrium point:

Case 1: $(u_0^*, v_0^*) = (1, 0)$ At this equilibrium point, the Jacobian matrix becomes diagonal:

$$J_i(u_0^*, v_0^*) = \begin{pmatrix} -\frac{\nu_1}{\delta^2}\theta_i - P & 0 \\ 0 & -\frac{\nu_2}{\delta^2}\theta_i - (P + \delta) \end{pmatrix}.$$

The eigenvalues of this matrix are:

$$\lambda_1 = -\frac{\nu_1}{\delta^2}\theta_i - P, \quad \lambda_2 = -\frac{\nu_2}{\delta^2}\theta_i - (P + \delta).$$

Since $\theta_i > 0$, the eigenvalues are negative if:

$$\frac{\nu_1}{\delta^2}\theta_i - P < 0, \quad \text{and} \quad \frac{\nu_2}{\delta^2}\theta_i - (P + \delta) < 0.$$

If these conditions hold, then both eigenvalues lie in the left half of the complex plane, ensuring that the equilibrium is locally asymptotically stable.

Case 2: $(u_1^*, v_1^*) = \left(\frac{2\eta}{P + \sigma}, \frac{P + \sigma}{2\eta}\right)$ At this equilibrium point, the Jacobian matrix becomes:

$$J_i(u_1^*, v_1^*) = \begin{pmatrix} -\frac{\nu_1}{\delta^2}\theta_i - a & -2 \\ -a & \frac{\nu_2}{\delta^2}\theta_i - \eta + 2 \end{pmatrix}, \quad \text{where} \quad a = \frac{P^2 + P\sigma}{2\eta^2}.$$

Let the trace and determinant of this matrix be:

$$\text{tr} = \left(\frac{\nu_1 + \nu_2}{\delta^2}\right)\theta_i - a - \eta + 2,$$

$$\det = \frac{\nu_1 \nu_2}{\delta^4}\theta_i^2 + \left(\frac{\nu_1}{\delta^2}(-\eta + 2) - \frac{\nu_2}{\delta^2}a\right)\theta_i + 2a.$$

Let Δ be the discriminant of the characteristic polynomial:

$$\Delta = (\text{tr})^2 - 4\det.$$

Now we consider two cases:

- If $\Delta > 0$, the eigenvalues are real and given by:

$$\lambda_{1,2} = \frac{\text{tr} \pm \sqrt{\Delta}}{2}.$$

  If in addition $\text{tr} < 0$ and $\det > 0$, then both eigenvalues are negative, and the equilibrium is asymptotically stable.
- If $\Delta < 0$, the eigenvalues are complex conjugates with:

$$\lambda_{1,2} = \frac{\text{tr}}{2} \pm i\frac{\sqrt{-\Delta}}{2}.$$

  Stability requires the real part of each eigenvalue to be negative, which is equivalent to $\text{tr} < 0$. Moreover, in the case of fractional-order systems, the stability condition requires that:

$$\text{Arg}(\lambda_j(\theta_i)) > \frac{\alpha\pi}{2}, \quad j = 1, 2,$$

  which ensures that the solution decays in the Mittag-Leffler sense for Caputo-type derivatives.

Case 3: $(u_2^*, v_2^*) = \left(\frac{2\eta}{P-\sigma}, \frac{P-\sigma}{2\eta}\right)$ In this case, the Jacobian becomes:

$$J_i(u_2^*, v_2^*) = \begin{pmatrix} -\frac{\nu_1}{\delta^2}\theta_i - b & -2 \\ -b & \frac{\nu_2}{\delta^2}\theta_i - \eta + 2 \end{pmatrix}, \quad \text{where} \quad b = \frac{P^2 - P\sigma}{2\eta^2}.$$

Then:

$$\text{tr} = \left(\frac{\nu_1 + \nu_2}{\delta^2}\right)\theta_i - b - \eta + 2,$$

$$\det = \frac{\nu_1\nu_2}{\delta^4}\theta_i^2 + \left(\frac{\nu_1}{\delta^2}(-\eta + 2) - \frac{\nu_2}{\delta^2}b\right)\theta_i + 2b.$$

As in the previous case, the discriminant is:

$$\Delta^* = (\text{tr})^2 - 4\det.$$

Again, we consider two subcases:

- If $\Delta^* > 0$, and $\text{tr} < 0$, $\det > 0$, then both eigenvalues are negative, and the equilibrium is stable.
- If $\Delta^* < 0$, the eigenvalues are complex conjugates. The real part is $\text{tr}/2$, so we require:

$$\text{tr} < 0 \quad \text{and} \quad \text{Arg}(\lambda_j(\theta_i)) > \frac{\alpha\pi}{2}.$$

Thus, in all cases, the stability of the equilibrium point is determined by evaluating the sign of the trace and determinant (or discriminant), and by checking that the eigenvalues lie inside the stability region defined by the argument condition for fractional-order systems. □

3. Global stability

In this section, we develop a Lyapunov function approach to analyze the global asymptotic stability of the system given in Eq (2.8).

Theorem 3. System (2.8) is globally asymptotically stable if

$$\min\left\{u^*v^{*2} + Pu^*,\ Pu^*,\ u^*v^{*2},\ (P+\delta)v^* - u^*v^{*2},\ (P+\delta)v^*\right\} > 0. \tag{3.1}$$

Proof. Define the Lyapunov functionals:

$$V_1(t) = \sum_{i,j} u^* L\left(\frac{u_{i,j}(t+\alpha h)}{u^*}\right), \quad V_2(t) = \sum_{i,j} v^* L\left(\frac{v_{i,j}(t+\alpha h)}{v^*}\right), \tag{3.2}$$

where $L(x) = x - \ln x - 1$ is the classical convex Lyapunov function. The total Lyapunov functional is given by:

$$V(t) = V_1(t) + V_2(t). \tag{3.3}$$

Assuming $u^* \neq 0$, $v^* \neq 0$, and applying the discrete fractional Caputo operator ${}_{C_h}\nabla_t^{\alpha}$, we compute:

$$\begin{aligned} {}_{C_h}\nabla_t^{\alpha} V_1(t) \leq \sum_{i,j}\left(1 - \frac{u^*}{u_{i,j}(t+\alpha h)}\right)\Bigg[u^*v^{*2}\left(1 - \frac{u_{i,j}(t+\alpha h)v_{i,j}^2(t+\alpha h)}{u^*v^{*2}}\right) \\ + Pu^*\left(1 - \frac{u_{i,j}(t+\alpha h)}{u^*}\right)\Bigg]. \end{aligned} \tag{3.4}$$

Using the identity $(1 - x^{-1})(1 - x) = -L(x^{-1}) - L(x)$, this simplifies to:

$$\begin{aligned} {}_{C_h}\nabla_t^{\alpha} V_1(t) \leq u^*v^{*2} \sum_{i,j}\left[-L\left(\frac{u^*}{u_{i,j}(t+\alpha h)}\right) - L\left(\frac{u_{i,j}(t+\alpha h)v_{i,j}^2(t+\alpha h)}{u^*v^{*2}}\right) + L\left(\frac{v_{i,j}^2(t+\alpha h)}{v^{*2}}\right)\right] \\ + Pu^* \sum_{i,j}\left[-L\left(\frac{u^*}{u_{i,j}(t+\alpha h)}\right) - L\left(\frac{u_{i,j}(t+\alpha h)}{u^*}\right)\right]. \end{aligned} \tag{3.5}$$

Similarly, we compute the derivative of $V_2(t)$:

$$\begin{aligned} {}_{C_h}\nabla_t^{\alpha} V_2(t) \leq \sum_{i,j}\left(1 - \frac{v^*}{v_{i,j}(t+\alpha h)}\right)\Bigg[-u^*v^{*2}\left(1 - \frac{u_{i,j}(t+\alpha h)v_{i,j}^2(t+\alpha h)}{u^*v^{*2}}\right) \\ + (P+\delta)v^*\left(1 - \frac{v_{i,j}(t+\alpha h)}{v^*}\right)\Bigg]. \end{aligned} \tag{3.6}$$

This simplifies to:

$$\begin{aligned} {}_{C_h}\nabla_t^{\alpha} V_2(t) \leq \sum_{i,j}\Bigg[-u^*v^{*2}L\left(\frac{v^*}{v_{i,j}(t+\alpha h)}\right) - L\left(\frac{u_{i,j}(t+\alpha h)v_{i,j}^2(t+\alpha h)}{u^*v^{*2}}\right) \\ + L\left(\frac{u_{i,j}(t+\alpha h)v_{i,j}(t+\alpha h)}{u^*v^*}\right) - (P+\delta)v^*\left(L\left(\frac{v^*}{v_{i,j}(t+\alpha h)}\right) + L\left(\frac{v_{i,j}(t+\alpha h)}{v^*}\right)\right)\Bigg]. \end{aligned} \tag{3.7}$$

Adding both expressions gives:

$$C_h\nabla_t^\alpha V(t) = C_h\nabla_t^\alpha V_1(t) + C_h\nabla_t^\alpha V_2(t), \tag{3.8}$$

$$\begin{aligned} C_h\nabla_t^\alpha V(t) \le \sum_{i,j}\Big[&-(u^*v^{*2} + Pu^*)L\left(\frac{u^*}{u_{i,j}(t+\alpha h)}\right) - Pu^*L\left(\frac{u_{i,j}(t+\alpha h)}{u^*}\right) \\ &-\Big((P+\delta)v^* - u^*v^{*2}\Big)L\left(\frac{v^*}{v_{i,j}(t+\alpha h)}\right) - (P+\delta)v^*L\left(\frac{v_{i,j}(t+\alpha h)}{v^*}\right) \\ &- u^*v^{*2}L\left(\frac{u_{i,j}(t+\alpha h)v_{i,j}(t+\alpha h)}{u^*v^*}\right)\Big]. \end{aligned} \tag{3.9}$$

Define

$$\xi := \min\left\{u^*v^{*2} + Pu^*,\ Pu^*,\ u^*v^{*2},\ (P+\delta)v^* - u^*v^{*2},\ (P+\delta)v^*\right\}.$$

If $\xi > 0$, then all the terms in the summation are negative, and we obtain:

$$C_h\nabla_t^\alpha V(t) \le 0.$$

This shows that the Lyapunov functional $V(t)$ is non-increasing. Since $V(t) \ge 0$, and the derivative is non-positive, it follows by Lyapunov's direct method that the solution converges to the equilibrium point. Hence, the system is globally asymptotically stable. □

4. Description of the numerical scheme

To confirm the theoretical stability analysis results presented in the previous section, we solve the model equation (1.2) numerically. The spatial part of the solution uses Chebyshev polynomials and Chebyshev–Gauss–Lobatto collocation points, which are distributed optimally within the interval $[-1, 1]$ to provide high accuracy, especially near the boundaries. For this, let $x_j = \cos\left(\frac{j\pi}{N}\right)$ and $y_m = \cos\left(\frac{m\pi}{M}\right)$ be the Chebyshev collocation points. The spatial derivatives are approximated using Chebyshev derivative matrices of the form:

$$u(x, y, t) \approx \sum_{i=0}^{N_x}\sum_{j=0}^{N_y} u_{ij}(t)T_i(x)T_j(y),$$

$$v(x, y, t) \approx \sum_{i=0}^{N_x}\sum_{j=0}^{N_y} v_{ij}(t)T_i(x)T_j(y),$$

where $T_i(x)$ and $T_j(y)$ are the Chebyshev polynomials of degree i and j. $u_{ij}(t)$ and $v_{ij}(t)$ are the spectral coefficients that depend on time t. N_x and N_y are the number of Chebyshev polynomials used for the approximation in the x- and y-directions. The derivatives of u and v with respect to x and y at the collocation points can be computed using Chebyshev derivative matrices.

For the first derivative, the entries of the Chebyshev first derivative matrix D_x are given by:

$$D_{jk} = \frac{c_j}{c_k}\frac{(-1)^{j+k}}{x_j - x_k}, \quad j \ne k,$$

where $c_0 = c_N = 2$, and $c_j = 1$ for $1 \leq j \leq N-1$. The diagonal elements of D_x are:

$$D_{jj} = -\frac{x_j}{2(1-x_j^2)}, \quad j = 1, 2, \ldots, N-1,$$

with special cases for $j = 0$ and $j = N$ given by

$$D_{00} = \frac{2N^2+1}{6}, \quad D_{NN} = -\frac{2N^2+1}{6}.$$

To compute the second derivatives, we construct the second derivative matrix D_x^2 by squaring the first derivative matrix:

$$D_x^2 = D_x \cdot D_x.$$

Similarly, for the y-direction, we construct the matrix D_y^2 for second derivatives with respect to y. Thus, the second derivatives of u and v at the collocation points are approximated as

$$\frac{\partial^2 u}{\partial x^2} \approx D_x^2 u, \quad \frac{\partial^2 u}{\partial y^2} \approx D_y^2 u,$$
$$\frac{\partial^2 v}{\partial x^2} \approx D_x^2 v, \quad \frac{\partial^2 v}{\partial y^2} \approx D_y^2 v.$$

For the fractional-order time derivative involved in the model equation (1.2), we apply the $L1$ scheme to discretize it. For this purpose, the Caputo fractional derivative of order $\alpha \in (0,1)$ is defined as

$$C_0\mathcal{D}_t^\alpha u(t) = \frac{1}{\Gamma(1-\alpha)} \int_0^t \frac{u'(s)}{(t-s)^\alpha}\, ds.$$

The $L1$ scheme provides a finite difference approximation of this derivative. For a uniform time step Δt, the Caputo fractional derivative at time $t_n = n\Delta t$ is approximated by

$$C_0\mathcal{D}_t^\alpha u(t_n) \approx \frac{1}{\Gamma(2-\alpha)} \sum_{k=0}^{n-1} a_k^\alpha \left(u(t_{n-k}) - u(t_{n-k-1})\right),$$

where the coefficients a_k^α are given by

$$a_k^\alpha = (k+1)^{1-\alpha} - k^{1-\alpha}.$$

By applying the Chebyshev spectral method for spatial discretization and the $L1$ scheme for temporal discretization, the resulting discrete formulation of the 2D reaction-diffusion system described in Eq (1.2) takes the following form:

$$\begin{aligned}
&\tfrac{1}{\Gamma(2-\alpha)} \sum_{k=0}^{n-1} a_k^\alpha \left(u_{ij}^{n-k} - U_{ij}^{n-k-1}\right) = \nu_1 \left((D_x^2 u^n)_{ij} + (D_y^2 u^n)_{ij}\right) - U_{ij}^n (v_{ij}^n)^2 + P(1-u_{ij}^n), \\
&\tfrac{1}{\Gamma(2-\alpha)} \sum_{k=0}^{n-1} a_k^\alpha \left(v_{ij}^{n-k} - v_{ij}^{n-k-1}\right) = \nu_2 \left((D_x^2 v^n)_{ij} + (D_y^2 v^n)_{ij}\right) + u_{ij}^n (v_{ij}^n)^2 - (P+\delta) v_{ij}^n.
\end{aligned} \tag{4.1}$$

5. Results and discussion

This section presents the results of numerical simulations for the fractional-in-time Gray–Scott reaction-diffusion model in two spatial dimensions. The results are analyzed in close connection with the theoretical conditions for local and global stability presented in Theorems 1–3. Specifically, we examine how diffusion destabilizes equilibria, the emergence and development of patterns, and how global asymptotic behavior relates to the structure of the Lyapunov function.

Example 1

Consider the parameters $\alpha = 0.7$, $\nu_1 = 0.01$, $\nu_2 = 0.02$, $P = 0.38$, and $\delta = 0.3$, along with zero-flux boundary conditions. The initial conditions are given by:

$$u(x, y, 0) = 5\sin(x)\sin(y), \quad v(x, y, 0) = e^{-x}e^{-y}.$$

The steady state of interest is the trivial homogeneous equilibrium $(u^*, v^*) = (1, 0)$, guarantees that this equilibrium is locally asymptotically stable in the absence of diffusion, whose eigenvalues are $\lambda_1 = -P < 0$ and $\lambda_2 = -(P + \delta) < 0$, confirming linear stability to homogeneous perturbations by Theorem 1. However, when diffusion is introduced, the system becomes susceptible to Turing-type instability, as detailed in Theorem 2. Stability is lost when there exists at least one spatial eigenvalue θ_i such that:

$$\frac{\nu_1}{\delta^2}\theta_i > P \quad \text{or} \quad \frac{\nu_2}{\delta^2}\theta_i > (P + \delta).$$

These inequalities describe diffusion-driven destabilization of the steady state through spatially nonuniform modes. Since ν_1 and ν_2 are small but non-zero, and $\delta = 0.3$, certain mid-range modes may become unstable, leading to pattern amplification.

Numerical simulations illustrate this effect. In Figure 1, small modulations appear, representing the activation of unstable eigenmodes. These spatial oscillations become more pronounced in Figures 2 and 3, where stripe-like structures begin to organize. By Figure 4, the pattern becomes highly irregular and chaotic, indicating that multiple unstable modes have grown and begun to interact nonlinearly, producing complex spatiotemporal behavior.

According to Theorem 3, global asymptotic stability is ensured if the following Lyapunov condition holds:

$$\min\left\{u^*v^{*2} + Pu^*,\ Pu^*,\ u^*v^{*2},\ (P + \delta)v^* - u^*v^{*2},\ (P + \delta)v^*\right\} > 0.$$

For the equilibrium $(1, 0)$, we have $v^* = 0$, which causes several of these terms to vanish. The minimum value is thus zero, violating the strict inequality. Consequently, the Lyapunov function $V(t)$ constructed in the proof of Theorem 3 is non-increasing but not strictly decreasing. This implies that the system may not converge to equilibrium. Instead, as seen in the simulation, the solution evolves into a long-lived, irregular, non-homogeneous pattern.

These results highlight the role of diffusion in destabilizing an otherwise stable equilibrium, leading to the emergence of complex patterns. The lack of global stability allows these structures to persist indefinitely, governed by the fractional time dynamics.

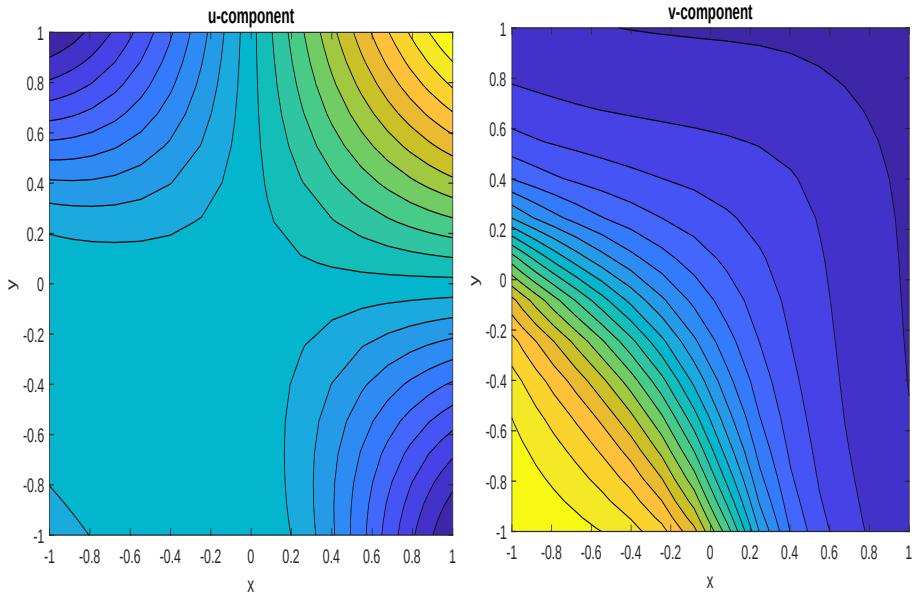

Figure 1. Example 1: Concentration of u and v at time step $\Delta t = 25$.

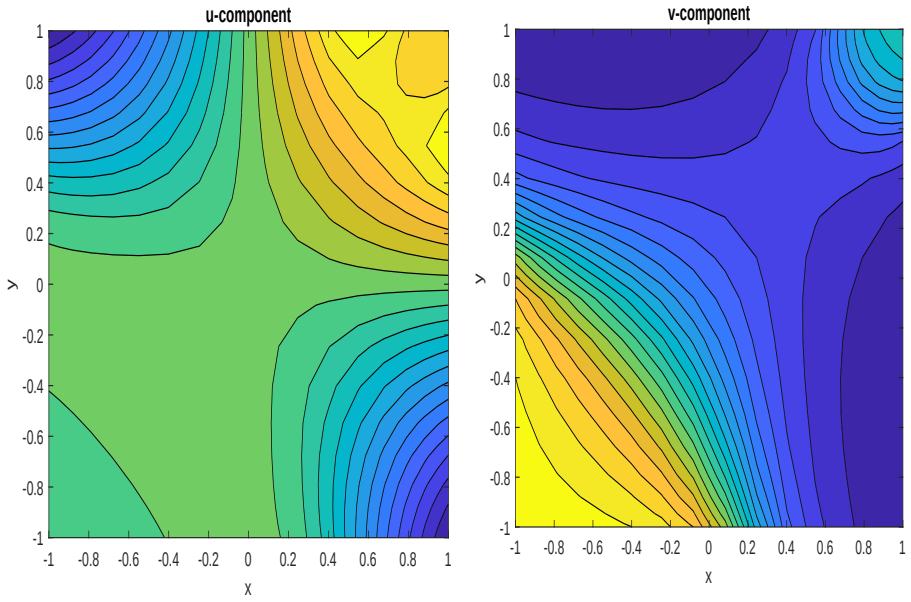

Figure 2. Example 1: Concentration of u and v at time step $\Delta t = 50$.

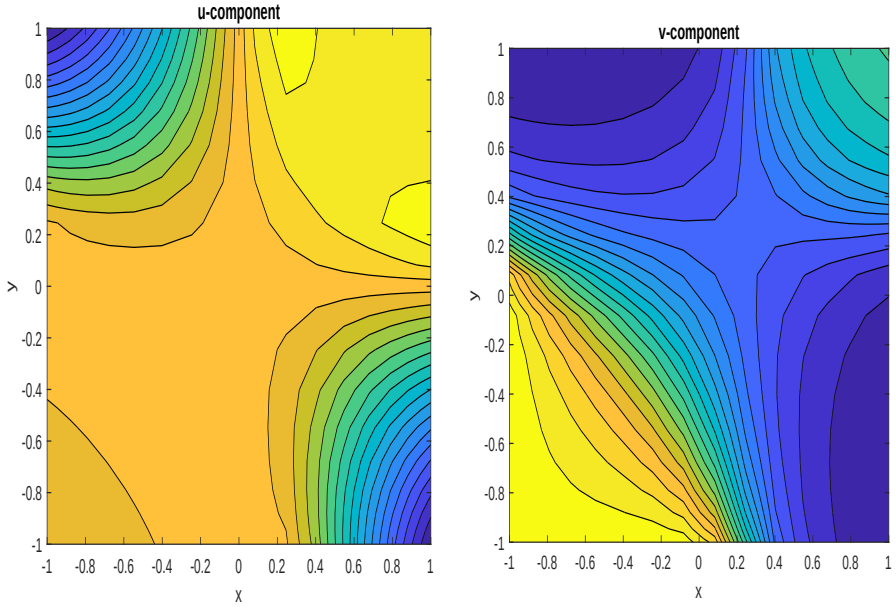

Figure 3. Example 1: Concentration of u and v at time step $\Delta t = 100$.

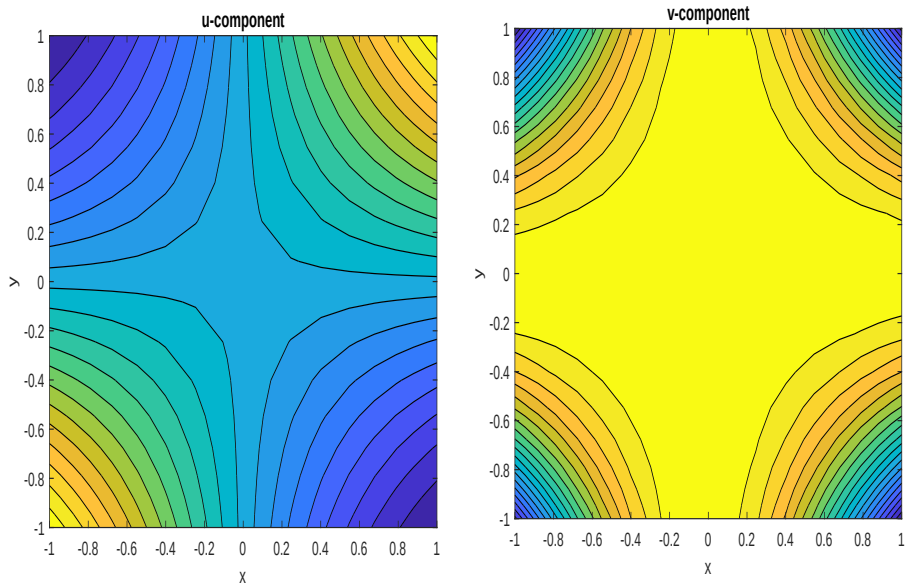

Figure 4. Example 1: Concentration of u and v at time step $\Delta t = 500$.

Example 2

In this second case, we consider a different parameter regime: $\alpha = 0.7$, $\nu_1 = \nu_2 = 0.001$, $P = 0.1$, and $\delta = 0.05$. The initial conditions are:

$$u(x, y, 0) = \cos(2\pi x)\cos(2\pi y), \quad v(x, y, 0) = \sin(2\pi x)\sin(2\pi y).$$

This configuration is designed to activate multiple spatial modes through the initial conditions while exploring a regime with very low diffusion and a small feed rate P.

In this case, the system admits a positive steady state (u^*, v^*) with both components strictly positive. Theorem 1 confirms local asymptotic stability of this equilibrium in the absence of diffusion, as the Jacobian matrix evaluated at (u^*, v^*) has eigenvalues with negative real parts. According to Theorem 2, the addition of diffusion allows for the growth of certain spatial eigenmodes when: $\mathrm{Re}(\lambda_j(\theta_i)) > 0 \quad \text{for some } \theta_i$.

However, due to the very small values of ν_1 and ν_2, only a narrow range of modes can become unstable, and the instability remains well-controlled. This is observed in Figure 5, where localized spot-like disturbances begin to form. In Figure 6, the solution develops well-defined and isolated spots. These structures remain stationary in Figures 7 and 8, indicating that the system has settled into a globally stable patterned attractor. Theorem 3 applies directly in this case. Since $u^* > 0$ and $v^* > 0$, all components of the Lyapunov condition $\min\left\{u^*v^{*2} + Pu^*,\ Pu^*,\ u^*v^{*2},\ (P+\delta)v^* - u^*v^{*2},\ (P+\delta)v^*\right\}$ are strictly positive. This ensures that the Lyapunov function $V(t)$ is strictly decreasing and the solution converges globally to the steady state. The numerical results confirm this prediction. After the transient development of spots, the solution exhibits no further oscillations or spatial changes, consistent with global asymptotic stability.

The above two examples showcase the contrasting dynamical behaviors dictated by Theorems 1–3. In Example 1, although the homogeneous equilibrium is locally stable without diffusion, the inclusion of spatial diffusion leads to instability (Theorem 2), and global stability is not achieved (Theorem 3). This results in the emergence of persistent, irregular spatiotemporal patterns. In contrast, Example 2 satisfies all stability conditions: Local stability, controlled diffusion-induced pattern formation, and global asymptotic convergence to a steady pattern.

The fractional time derivative with $\alpha = 0.7$ plays a fundamental role in both cases. The memory effects inherent in the Caputo derivative slow the temporal evolution, allowing smoother pattern transitions and long-lived structures. This behavior is essential for modeling real-world systems with nonlocal temporal effects, such as chemical reaction kinetics and biological diffusion processes.

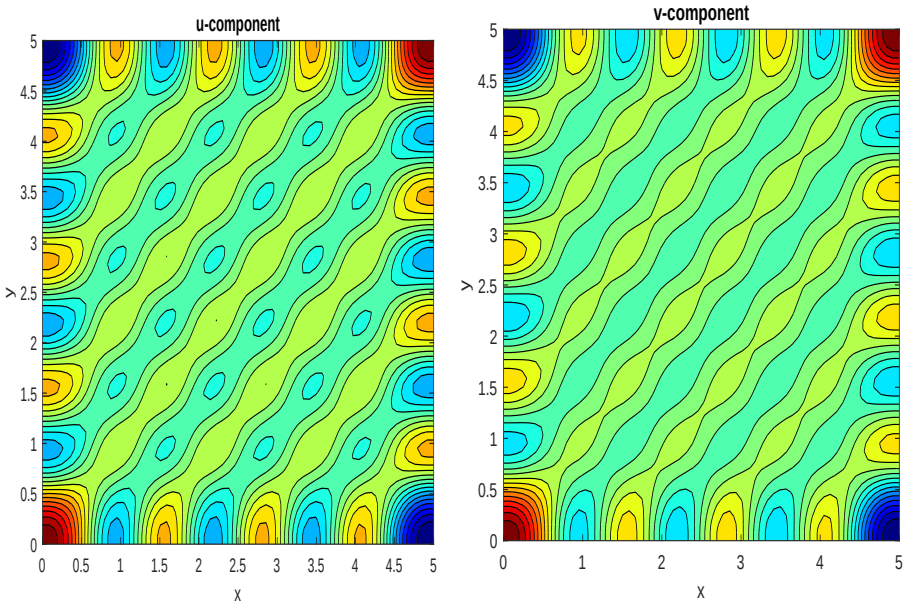

Figure 5. Example 2: Concentration of u and v at time step $\Delta t = 10$.

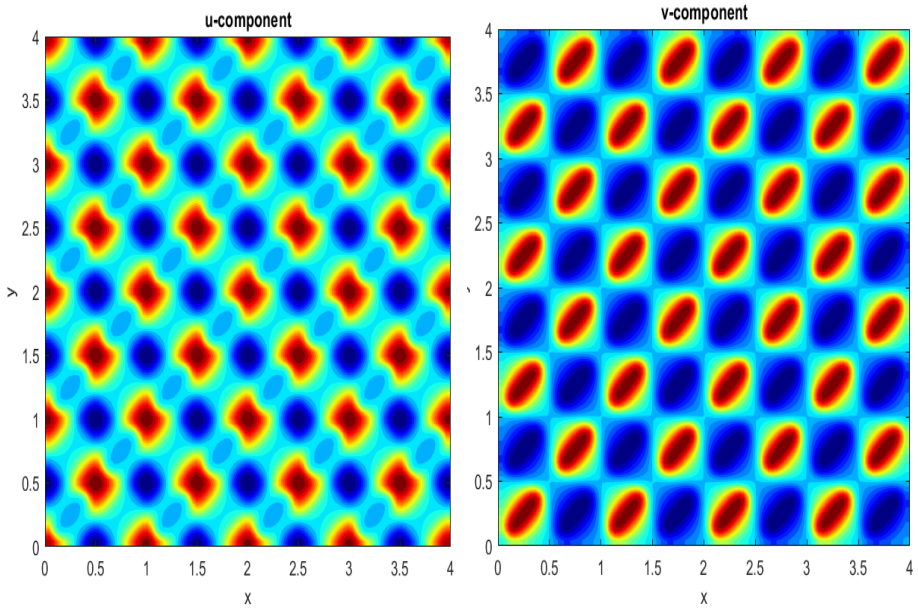

Figure 6. Example 2: Concentration of u and v at time step $\Delta t = 500$.

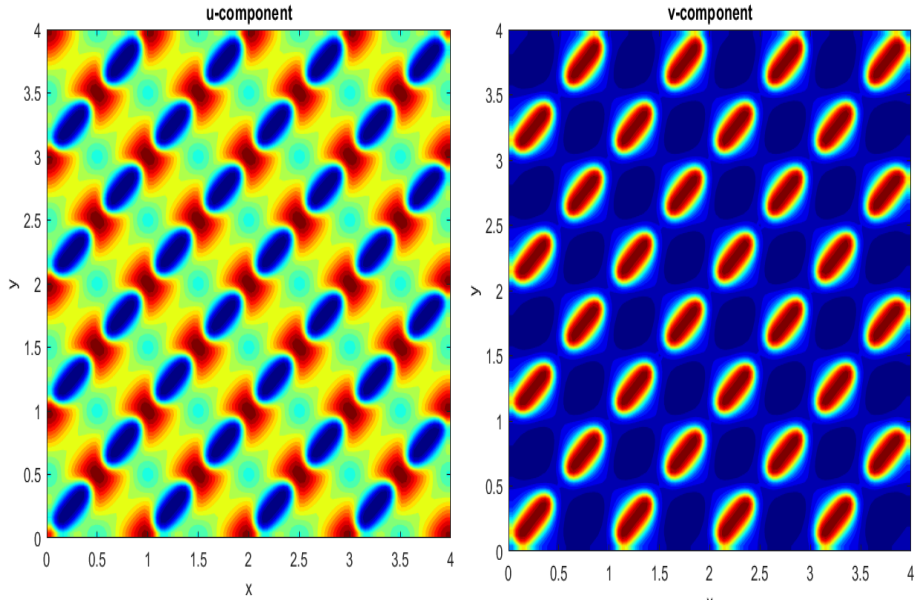

Figure 7. Example 2: Concentration of u and v at time step $\Delta t = 1500$.

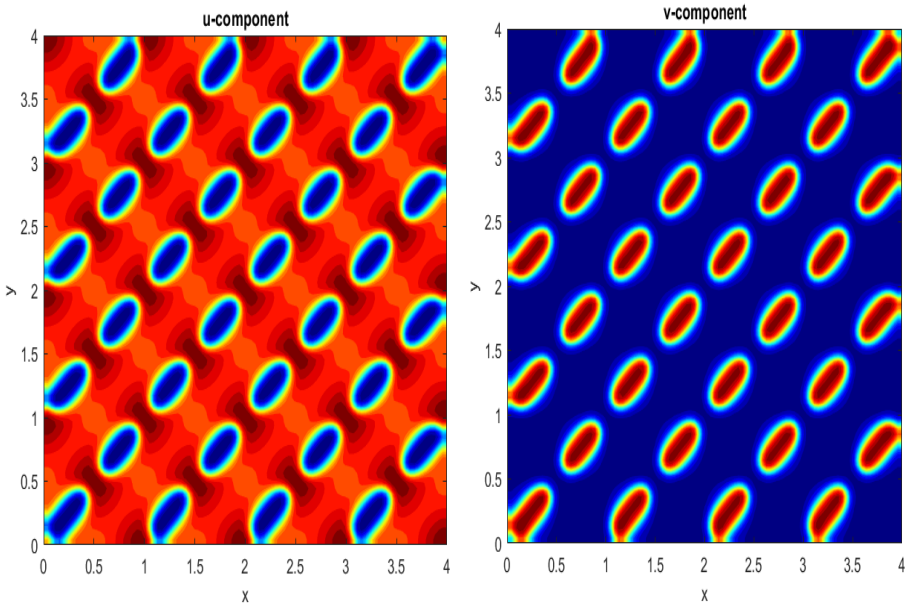

Figure 8. Example 2: Concentration of u and v at time step $\Delta t = 2500$.

6. Conclusions

In this research work, we investigated the local and global stability of the fractional in-time Gray–Scott reaction-diffusion model using the Caputo fractional derivative. Through both theoretical analysis and numerical simulations, the model demonstrated complex spatio-temporal behaviors and pattern formations. Our results show how incorporating a Caputo time-fractional derivative and a non-integer diffusion framework affects system dynamics. In particular, eigenvalue analysis of the linearized system and construction of Lyapunov functionals yield clear criteria for local and global stability of the homogeneous steady state. By employing the Chebyshev spectral method for spatial discretization and the $L1$ scheme for fractional time derivatives, we achieved a highly accurate representation of the system's dynamics. Our results validated the model's ability to capture phenomena such as Turing patterns and self-replicating spots, showcasing the potential of fractional derivatives in enhancing the understanding of reaction-diffusion processes.

Author contributions

Ishtiaq Ali: Methodology, conceptualization, validation writing-original draft preparation, resources; Saeed Islam: Methodology, investigation, formal analysis, visualization, reviewing, editing. All authors have read and approved the final version of the manuscript for publication.

Use of Generative-AI tools declaration

The authors declare they have not used Artificial Intelligence (AI) tools in the creation of this article.

Funding

This work was supported by the Deanship of Scientific Research, Vice Presidency for Graduate Studies and Scientific Research, King Faisal University, Saudi Arabia [Grant No. KFU251966].

Conflicts of interest

The authors declare no conflict of interest.

References

1. B. Baeumer, M. Kovács, M. M. Meerschaert, Numerical solutions for fractional reaction-diffusion equations, *Comput. Math. Appl.*, **55** (2008), 2212–2226. https://doi.org/10.1016/j.camwa.2007.11.012
2. A. Ghafoor, M. Fiaz, M. Hussain, A. Ullah, E. A. A. Ismail, F. A. Awwad, Dynamics of the time-fractional reaction-diffusion coupled equations in biological and chemical processes, *Sci. Rep.*, **14** (2024), 7549. https://doi.org/10.1038/s41598-024-58073-z
3. A. El Hassani, K. Hattaf, N. Achtaich, Global stability of reaction-diffusion equations with fractional Laplacian operator and applications in biology, *Commun. Math. Biol. Neurosci.*, **2022** (2022), 56. https://doi.org/10.28919/cmbn/7485
4. T. Wang, F. Song, H. Wang, G. E. Karniadakis, Fractional Gray–Scott model: Well-posedness, discretization, and simulations, *Comput. Methods Appl. Mech. Eng.*, **347** (2019), 1030–1049. https://doi.org/10.1016/j.cma.2019.01.002
5. K. J. Lee, W. D. McCormick, J. E. Pearson, H. L. Swinney, Experimental observation of self-replicating spots in a reaction–diffusion system, *Nature*, **369** (1994), 215–218. https://doi.org/10.1038/369215a0
6. A. M. Turing, The chemical basis of morphogenesis, *Philos. Trans. R. Soc. Lond. B Biol. Sci.*, **237** (1952), 37–72. https://doi.org/10.1098/rstb.1952.0012
7. V. Castets, E. Dulos, J. Boissonade, P. De Kepper, Experimental evidence of a sustained standing Turing-type nonequilibrium chemical pattern, *Phys. Rev. Lett.*, **64** (1990), 2953–2965. https://doi.org/10.1103/PhysRevLett.64.2953
8. Q. Ouyang, H. L. Swinney, Transition from a uniform state to chemical patterns in a reaction-diffusion system, *Nature*, **352** (1991), 610–612. https://doi.org/10.1038/352610a0
9. L. Xu, L. J. Zhao, Z. X. Chang, J. T. Feng, Turing instability and pattern formation in a semi-discrete Brusselator model, *Mod. Phys. Lett. B*, **27** (2013), 1350006. https://doi.org/10.1142/S0217984913500061
10. W. Mazin, K. E. Rasmussen, E. Mosekilde, P. Borckmans, Pattern formation in the bistable Gray–Scott model, *Math. Comput. Simul.*, **40** (1996), 371–396. https://doi.org/10.1016/0378-4754(95)00044-5
11. O. Ersoy, I. Dağ, Numerical solutions of the reaction-diffusion system by using exponential cubic B-spline collocation algorithms, *Open Phys.*, **13** (2015), 153–158. https://doi.org/10.1515/phys-2015-0047

12. A. T. Onarcan, N. Adar, I. Dağ, Trigonometric cubic B-spline collocation algorithm for numerical solutions of reaction-diffusion equation systems, *Comput. Appl. Math.*, **37** (2018), 6848–6869. https://doi.org/10.1007/s40314-018-0713-4
13. C. S. Chou, Y. T. Zhang, R. Zhao, Q. Nie, Numerical methods for stiff reaction-diffusion systems, *Discrete Contin. Dyn. Syst. Ser. B*, **7** (2007), 515–525. https://doi.org/10.3934/dcdsb.2007.7.515
14. E. Özuğurlu, A note on the numerical approach for the reaction-diffusion problem to model the density of the tumor growth dynamics, *Comput. Math. Appl.*, **69** (2015), 1504–1517. https://doi.org/10.1016/j.camwa.2015.04.018
15. A. Madzvamuse, A. H. Chung, The bulk-surface finite element method for reaction-diffusion systems on stationary volumes, *Finite Elem. Anal. Des.*, **108** (2016), 9–21. https://doi.org/10.1016/j.finel.2015.09.002
16. R. Mittal, R. Jiwari, Numerical study of two-dimensional reaction-diffusion Brusselator system by differential quadrature method, *Int. J. Comput. Methods Eng. Sci. Mech.*, **12** (2011), 14–25. https://doi.org/10.1080/15502287.2010.540300
17. P. Gray, S. K. Scott, Autocatalytic reactions in the isothermal, continuous stirred tank reactor: Oscillations and instabilities in the system $A + 2B \rightarrow 3B$, $B \rightarrow C$, *Chem. Eng. Sci.*, **39** (1984), 1087–1097. https://doi.org/10.1016/0009-2509(84)87017-7
18. P. Gray, S. K. Scott, *Chemical oscillations and instabilities*, Oxford University Press, Oxford, 1990.
19. E. E. Selkov, Self-oscillations in glycolysis, *Eur. J. Biochem.*, **4** (1968), 79–86. https://doi.org/10.1111/j.1432-1033.1968.tb00175.x
20. J. E. Pearson, Complex patterns in a simple system, *Science*, **261** (1993), 189–192. https://doi.org/10.1126/science.261.5118.189
21. S. Aljhani, M. S. Md Noorani, K. M. Saad, A. K. Alomari, Numerical solutions of certain new models of the time-fractional Gray–Scott, *J. Funct. Spaces*, **2021** (2021), 2544688. https://doi.org/10.1155/2021/2544688
22. J. S. McGough, K. Riley, Pattern formation in the Gray–Scott model, *Nonlinear Anal. Real World Appl.*, **5** (2004), 105–121. https://doi.org/10.1016/S1468-1218(03)00020-8
23. I. Podlubny, *Fractional differential equations: An introduction to fractional derivatives, fractional differential equations, to methods of their solution and some of their applications*, Elsevier, San Diego, 1998.
24. R. Magin, Fractional calculus in bioengineering, part 1, *Crit. Rev. Biomed. Eng.*, **32** (2004), 1–104. https://doi.org/10.1615/CritRevBiomedEng.v32.i1.10
25. K. M. Owolabi, R. P. Agarwal, E. Pindza, S. Bernstein, M. S. Osman, Complex Turing patterns in chaotic dynamics of autocatalytic reactions with the Caputo fractional derivative, *Neural Comput. Appl.*, 2023, 1–27. https://doi.org/10.1007/s00521-023-08298-2
26. M. Alqhtani, K. M. Owolabi, K. M. Saad, E. Pindza, Spatiotemporal chaos in spatially extended fractional dynamical systems, *Commun. Nonlinear Sci. Numer. Simul.*, **119** (2023), 107118. https://doi.org/10.1016/j.cnsns.2023.107118
27. M. Alqhtani, K. M. Owolabi, K. M. Saad, Spatiotemporal (target) patterns in sub-diffusive predator-prey system with the Caputo operator, *Chaos Soliton. Fract.*, **160** (2022), 112267. https://doi.org/10.1016/j.chaos.2022.112267

28. K. M. Owolabi, E. Pindza, A. Atangana, Analysis and pattern formation scenarios in the superdiffusive system of predation described with Caputo operator, *Chaos Soliton. Fract.*, **152** (2021), 111468. https://doi.org/10.1016/j.chaos.2021.111468
29. K. M. Owolabi, B. Karaagac, D. Baleanu, Dynamics of pattern formation process in fractional-order super-diffusive processes: A computational approach, *Soft Comput.*, **25** (2021), 11191–11208. https://doi.org/10.1007/s00500-021-05885-0
30. K. M. Owolabi, D. Baleanu, Emergent patterns in diffusive Turing-like systems with fractional-order operator, *Neural Comput. Appl.*, **33** (2021), 12703–12720. https://doi.org/10.1007/s00521-021-05917-8
31. K. M. Owolabi, S. Jain, Spatial patterns through diffusion-driven instability in modified predator-prey models with chaotic behaviors, *Chaos Soliton. Fract.*, **174** (2023), 113839. https://doi.org/10.1016/j.chaos.2023.113839
32. K. M. Owolabi, K. C. Patidar, Higher-order time-stepping methods for time-dependent reaction–diffusion equations arising in biology, *Appl. Math. Comput.*, **240** (2014), 30–50. https://doi.org/10.1016/j.amc.2014.04.055
33. K. M. Owolabi, Mathematical analysis and numerical simulation of patterns in fractional and classical reaction–diffusion systems, *Chaos Soliton. Fract.*, **93** (2016), 89–98. https://doi.org/10.1016/j.chaos.2016.10.005
34. E. Pindza, K. M. Owolabi, Fourier spectral method for higher order space fractional reaction–diffusion equations, *Commun. Nonlinear Sci. Numer. Simul.*, **40** (2016), 112–128. https://doi.org/10.1016/j.cnsns.2016.04.020
35. K. J. Lee, H. L. Swinney, Lamellar structures and self-replicating spots in a reaction-diffusion system, *Phys. Rev. E*, **51** (1995), 1899–1915. https://doi.org/10.1103/PhysRevE.51.1899
36. K. J. Lin, W. D. McCormick, J. E. Pearson, H. L. Swinney, Experimental observation of self-replicating spots in a reaction-diffusion system, *Nature*, **369** (1994), 215–218. https://doi.org/10.1038/369215a0
37. B. Liu, R. Wu, N. Iqbal, L. Chen, Turing patterns in the Lengyel–Epstein system with super diffusion, *Int. J. Bifurcat. Chaos*, **27** (2017), 1730026. https://doi.org/10.1142/S0218127417300269
38. F. Liu, P. Zhuang, V. Anh, I. Turner, K. Burrage, Stability and convergence of the difference methods for the space–time fractional advection–diffusion equation, *Appl. Math. Comput.*, **191** (2007), 12–20. https://doi.org/10.1016/j.amc.2006.08.162
39. W. Mazin, K. E. Rasmussen, E. Mosekilde, P. Borckmans, G. Dewel, Pattern formation in the bistable Gray–Scott model, *Math. Comput. Simul.*, **40** (1996), 371–396. https://doi.org/10.1016/0378-4754(95)00044-5
40. J. S. McGough, K. Riley, Pattern formation in the Gray–Scott model, *Nonlinear Anal. Real World Appl.*, **5** (2004), 105–121. https://doi.org/10.1016/S1468-1218(03)00020-8
41. M. M. Meerschaert, C. Tadjeran, Finite difference approximations for two-sided space-fractional partial differential equations, *Appl. Numer. Math.*, **56** (2006), 80–90. https://doi.org/10.1016/j.apnum.2005.02.008
42. Z. Zhang, Q. Ouyang, Global existence, blow-up and optimal decay for a nonlinear viscoelastic equation with nonlinear damping and source term, *Discrete Contin. Dyn. Syst. Ser. B*, **28** (2023), 4735–4760. https://doi.org/10.3934/dcdsb.2023038

43. Z. Y. Zhang, Z. H. Liu, Y. J. Deng, J. H. Huang, C. X. Huang, Long time behavior of solutions to the damped forced generalized Ostrovsky equation below the energy space, *Proc. Amer. Math. Soc.*, **149** (2021), 1527–1542. https://doi.org/10.1090/proc/15322
44. Y. Wen, X. F. Zhou, Z. Zhang, S. Liu, Lyapunov method for nonlinear fractional differential systems with delay, *Nonlinear Dyn.*, **82** (2015), 1015–1025. https://doi.org/10.1007/s11071-015-2214-y
45. Y. Li, Y. Chen, I. Podlubny, Stability of fractional-order nonlinear dynamic systems: Lyapunov direct method and generalized Mittag-Leffler stability, *Comput. Math. Appl.*, **59** (2010), 1810–1821. https://doi.org/10.1016/j.camwa.2009.08.019
46. S. Liu, W. Jiang, X. Li, X. F. Zhou, Lyapunov stability analysis of fractional nonlinear systems, *Appl. Math. Lett.*, **51** (2016), 13–19. https://doi.org/10.1016/j.aml.2015.06.018
47. I. Ali, M. T. Saleem, Spatiotemporal dynamics of reaction–diffusion system and its application to Turing pattern formation in a Gray–Scott model, *Mathematics*, **11** (2023), 1459. https://doi.org/10.3390/math11061459
48. I. Ali, S. U. Khan, Threshold of stochastic SIRS epidemic model from infectious to susceptible class with saturated incidence rate using spectral method, *Symmetry*, **14** (2022), 1838. https://doi.org/10.3390/sym14091838
49. I. Ali, S. U. Khan, A dynamic competition analysis of stochastic fractional differential equation arising in finance via pseudospectral method, *Mathematics*, **11** (2023), 1328. https://doi.org/10.3390/math11061328
50. I. Ali, S. U. Khan, Dynamics and simulations of stochastic COVID-19 epidemic model using Legendre spectral collocation method, *AIMS Math.*, **8** (2023), 4220–4236. https://doi.org/10.3934/math.2023210
51. I. Ali, Dynamical analysis of two-dimensional fractional-order-in-time biological population model using Chebyshev spectral method, *Fractals Fract.*, **8** (2024), 325. https://doi.org/10.3390/fractalfract8060325
52. D. Gottlieb, S. A. Orszag, *Numerical analysis of spectral methods: Theory and applications*, SIAM, Philadelphia, PA, USA, 1977. https://doi.org/10.1137/1.9781611970425
53. J. C. Mason, D. C. Handscomb, *Chebyshev Polynomials*, CRC Press LLC, New York, NY, USA, 2003. https://doi.org/10.1201/9781420036114
54. C. Canuto, M. Y. Hussaini, A. Quarteroni, T. A. Zang, *Spectral Methods: Fundamentals in Single Domains*, Springer Series in Scientific Computation, Springer, New York, NY, USA, 2006. https://doi.org/10.1007/978-3-540-30726-6

AIMS Press